Available online at www.sciencedirect.com
ScienceDirect
Environmental Pollution 149 (2007) 31–43
ENVIRONMENTAL POLLUTION
www.elsevier.com/locate/envpol

Fluxes of oxidised and reduced nitrogen above a mixed coniferous forest exposed to various nitrogen emission sources

J. Neirynck [a,*], A.S. Kowalski [b], A. Carrara [c], G. Genouw [a], P. Berghmans [d], R. Ceulemans [e]

[a] Research Institute for Nature and Forest, Gaverstraat 4, B-9500 Geraardsbergen, Belgium
[b] Departamento de Física Aplicida, Facultad de Ciencias, Universidad de Granada, Calle Fuentenueva, SP-18071 Granada, Spain
[c] Fundacion CEAM, Parque Technologico, Calle Charles H. Darwin 14, SP-46980 Paterna (Valencia), Spain
[d] Flemish Institute for Technological Research, Boeretang 200, B-2400 Mol, Belgium
[e] Department of Biology, University of Antwerp, Universiteitsplein 1, B-2610 Wilrijk (Antwerp), Belgium

Received 1 February 2006; received in revised form 14 December 2006; accepted 17 December 2006

Reduced nitrogen was found to be the main contributor to total deposition which was predominantly governed by dry deposition.

Abstract

Concentrations of nitrogen gases (NH_3, NO_2, NO, HONO and HNO_3) and particles (pNH_4 and pNO_3) were measured over a mixed coniferous forest impacted by high nitrogen loads. Nitrogen dioxide (NO_2) represented the main nitrogen form, followed by nitric oxide (NO) and ammonia (NH_3). A combination of gradient method (NH_3 and NO_x) and resistance modelling techniques (HNO_3, HONO, pNH_4 and pNO_3) was used to calculate dry deposition of nitrogen compounds. Net flux of NH_3 amounted to -64 ng N m^{-2} s^{-1} over the measuring period. Net fluxes of NO_x were upward (8.5 ng N m^{-2} s^{-1}) with highest emission in the morning. Fluxes of other gases or aerosols substantially contributed to dry deposition. Total nitrogen deposition was estimated at -48 kg N ha^{-1} yr^{-1} and consisted for almost 80% of NH_x. Comparison of throughfall nitrogen with total deposition suggested substantial uptake of reduced N (± 15 kg N ha^{-1} yr^{-1}) within the canopy.

Keywords: Ammonia; Gradient method; Resistance model; Oxidised nitrogen; Throughfall

1. Introduction

Many forest ecosystems in Flanders are subjected to acidifying and eutrophicating nitrogen inputs. The presence of nitrogen emission sources and the fast removal of gases and aerosols from the atmosphere by enhanced turbulent transfer and the scavenging properties of the canopy lead to the delivery of considerable chemical doses to forests, which may affect their structure and functioning. Simple mass balance calculations for over 1400 forest receptor points in Flanders (1993–1998) indicated that modelled deposition largely exceeded critical loads related to protection of floral composition, safeguarding balanced nutrient supply and preventing groundwater contamination by nitrate leaching, especially at coniferous receptor sites (Neirynck et al., 2004). Not only does deposition of reduced and oxidised nitrogen contribute to acidification and eutrophication but their presence is also linked to other environmental issues such as photochemical air pollution (Fowler et al., 1998), radiative forcing (Adams et al., 2001) and visibility impairment (Barthelmie and Pryor, 1998).

Monitoring and modelling programmes have been launched to improve understanding and measurement of surface exchange of trace gases and particles (Erisman et al., 2005). Results are needed to allow the evaluation of abatement strategies and calculation of regional deposition budgets of atmospherically derived nitrogen (Butler et al., 2005; Fowler et al., 2005; Sutton et al., 2003).

* Corresponding author. Tel.: +32 054 437119; fax: +32 054 436161.
E-mail address: johan.neirynck@inbo.be (J. Neirynck).

0269-7491/$ - see front matter © 2007 Elsevier Ltd. All rights reserved.
doi:10.1016/j.envpol.2006.12.029

As an alternative to expensive and time-consuming micrometeorological measurements and resistance modelling, throughfall measurements are often used to determine the nitrogen flux in forests. This form of monitoring is cost-effective and was currently being carried out in more than 500 level II-plots across Europe (Lorenz et al., 2006). A significant drawback, however, is that throughfall underestimates total nitrogen flux, since a proportion of nitrogen may be taken up by the canopy or consumed by canopy-dwelling micro organisms (Lovett and Lindberg, 1993). Moreover, throughfall does not include the dry deposition flux of gases and fine aerosols directly to the soil (Lindberg et al., 1986).

This paper focuses on the presence and exchange properties of different oxidised and reduced nitrogen forms above mixed coniferous forest, exposed to nearby nitrogen emission sources. Fluxes of these compounds are obtained through a combination of gradient measurements and resistance modelling in order to obtain an insight into their relative contribution to the dry deposition flux. Additionally, dry and wet deposition fluxes are compared to throughfall nitrogen data in the forest in order to gain a clearer understanding of how throughfall samplers underestimate the total nitrogen flux.

2. Material and methods

2.1. Site description

The measurements are conducted over a mixed coniferous/deciduous forest located in the Campine region of Flanders (Belgium, 51°18′ N, 4°31′ E) approximately 15 km northeast of Antwerp. The forest encompasses over 300 ha, and is heterogeneous but of even height. The landscape is a coastal plain, with a gentle (0.3%) slope. The measurement site in the forest concerns a 2 ha large Scots pine stand (*Pinus sylvestris* L.) planted in 1929. Other Scots pine stands surround (ca. 150–300 m) the measurement site, with patches of deciduous trees found further away. It is bordered to the north and west by residential areas of the town of Brasschaat at a distance of ca. 500 m (Fig. 1), and to the south and east the forest extends over 2 km before turning into rural, partially forested terrain.

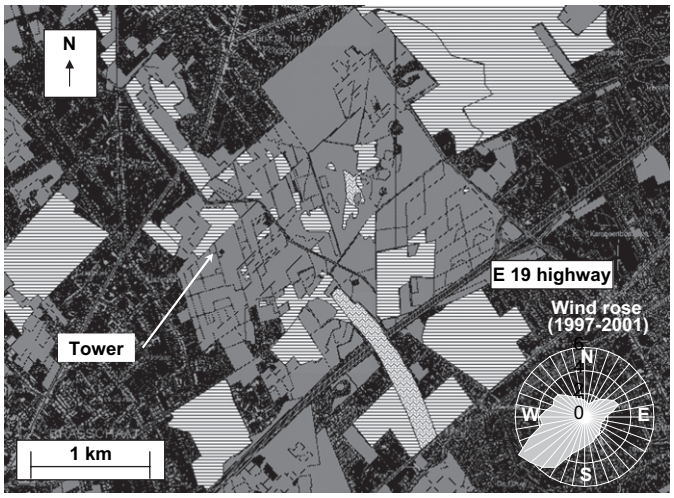

Fig. 1. Location of the measurement tower in the experimental forest site (grey: forest, black: residential areas, waves: water pools, horizontal bands: low vegetation types such as meadows, clearcuts or moorlands).

The forest is exposed to different pollution climates. Southerly to westerly winds bring SO_2 and NO_x-bearing air masses originating from either the petrochemical industry in the harbour of Antwerp (15 km to the west) or from E19 highway traffic (2 km to the south), suburban traffic and heating from contiguous buildings. Ammonia emission – from cattle stables and manure spreading – originates from rural communities located approximately 10 km north and east and the concerning grid cells have an emission flux density ranging between 4 and 11 t N km^{-2} yr^{-1}. Manure spreading also takes place within 5 km of the forest.

2.2. Meteorological measurements

A self-supporting welded square scaffolding tower was erected in the measuring site to a height of 40 m, with a 9 m^2 ground area and platforms at 9, 15, 18, 23, 31 and 39 m, next to a level II observation plot of the European ICP-Forests network (EC-UN/ECE, 1996), which also features in the CARBO-EUROPE IP research network (http://www.carboeurope.org). Meteorological data included vertical profiles of air temperature and humidity (psychrometer, Didcot DTS-5A, UK) at 2, 10, 24, 32 and 40 m and wind speed (cup anemometer, Didcot DWR-205G, UK) at 24, 32 and 40 m. At the top of the tower, measurements were made of down-welling shortwave radiation (pyranometer, Kipp and Zonen CM6B, The Netherlands), photosynthetic photon flux density (PPFD quantum sensor, JYP 1000, JDEC, France) and precipitation (tipping bucket, Didcot DRG-51, UK). A leaf wetness sensor (237F, Campbell, UK) was mounted on a boom at 19 m. All meteorological sensors were sampled at 0.1 Hz and stored as half hour means on a data logger (Campbell CR10, UK). A 3D sonic anemometer (model SOLENT 1012R2, Gill Instruments, UK) was deployed on a mast above the tower at 41 m.

2.3. Measurements of N compounds

2.3.1. Sampling and analysis of N-containing gases and particles in air

Measurements of gaseous NO_x (chemiluminescence, Ecophysics 700 AL, Switzerland, detection limit 1 ppb) and NH_3 (Conductivity, AMANDA, ECN, The Netherlands, detection limit 0.1 μg m^{-3}) were conducted at three levels above the canopy (23, 31 and 39 m) every half hour. For NO_x, air was drawn through heated Teflon tubing (35 °C) to the measuring unit at ground level. For NH_3, wet rotating annular denuders (Wyers et al., 1993) were deployed at the platforms to trap gaseous NH_3 into an acid solution ($NaHSO_4 \cdot H_2O$ 0.5 g/l) rotating in the denuders. The solution was transported from the denuders to a heated detection cell at the 23 m level platform. Ammonia gradients were only available for the period June 1999–November 2001. Gradient measurements of NO_x, discussed in this paper, applied to the same period.

Gases of nitrous acid (HONO), nitric acid (HNO_3) and fine particles of ammonium (pNH_4) and nitrate (pNO_3) were measured on a daily basis, in three separate sampling campaigns, during the time when the AMANDA analyser was operational. Daily measurements of NH_3 and pNH_4 were conducted by the Flemish Institute for Technological Research (Berghmans et al., 2001) between September 1999 and July 2000[1] using a glass honeycomb denuder–filter pack system (Koutrakis et al., 1993). The sampling cartridges consisted of a PTFE-coated $PM_{2.5}$ keyhole impactor, a glass transition section, two honeycomb denuders, a spacer, and a filter pack. The cartridges were attached to a sampling manifold and a sample changer deployed at the 24 m platform. This device controlled the flow through seven ports with attached cartridges, which were sampled consecutively starting from midnight onwards. Air was drawn at a rate of 10 L min^{-1} at which the impactor had a 50% cut point at 2.5 μm.

Denuders were coated with a methanol solution containing 1% glycerol and 2% citric acid to remove NH_3. Aerosols were caught on the filter pack deployed behind the denuder, which consisted of a Teflon filter (Teflon 47 mm, 2 μm, Pall–Gelman P/N R2PJ047) for particle collection and two additional quartz fibre filters (QF20 47 mm, Schleicher & Schuell Ref. No. 10373219) impregnated with a methanol solution of 2% citric acid and 2% glycerol to

[1] No measurements taken in January 2000 and additional daily measurements of NH_3 were taken in September/October 2000.

collect revolatilized NH_3 from the Teflon filters. After being coated, the denuders were immediately dried with clean dry air and capped to prevent contamination by NH_3. The cartridges were assembled in the laboratory and checked for leaks, before being transported to the sampling site.

The same setting was used to perform daily samplings of pNO_3, HONO and HNO_3, conducted in January–March 2001 (*winter campaign NO_y 2001*). Gases were collected on coated honeycomb denuders (coating solution of 50/50 methanol/ultrapure water with 1% glycerol and 1% Na_2CO_3). A nylon membrane filter (Nylasorb 47 mm 1.0 μm, Pall–Gelman P/N 66509) was used for collecting particles. Quartz fibre filters (QF20 47 mm, Schleicher & Schuell Ref. No. 10373219) with coating solutions of 2% glycerol and 1% Na_2CO_3 were positioned behind the nylon filter for absorbing evaporated acid gases produced from reactions at the nylon filter surface.

After sampling, the cartridges were transported to laboratory and dissembled under acid-aerosol-free conditions. For the NH_3 measurements, denuders were extracted with 10 mL of ultrapure water. The extraction solution for the HONO and HNO_3 denuder measurements included 0.239 g/L Na_2CO_3 and 0.235 g/L $NaHCO_3$ in deionised water. For the filter samples (pNH_4, pNO_3) an extraction volume of 20 mL was used. The samples were stored at 4 °C and usually analysed within 1 week. All sampling preparations were carried out in an acidic gas-free laminar flow box; the water met Millipore quality (conductivity < 0.05 μS cm^{-1}). The ionic concentrations of the aqueous extracts were determined using ion chromatography (Dionex 120-SE, separation columns AS14A for anions and CS12A for cations) under standard conditions. Accuracy was checked by certified standards (Spex IC Instrument Check Standard 6 (cat. No. ICMIX6-100) for anions and (Spex IC Instrument Check Standard 4 (cat. No. ICMIX4-100) for cations. The overall accuracy in IC analysis was around 5% for all analytes. Field blanks were taken every week during measurements. The procedural blanks were collected in the field with a passive exposure to air. Blank levels, typically ~1.5 μg for NH_3, ~2.3 μg for HNO_3 and ~1.7 μg for HONO, were subtracted from the detected amounts. The minimum detectable limits (defined as the standard deviation of the field blanks and based on an assumed mean air volume of 14.6 m^3) were (in μg m^{-3}) 0.07 for NH_3, 0.06 for HONO, 0.08 for HNO_3, 0.06 for pNH_4^+, and 0.09 for pNO_3^-. For the measurement of HONO and HNO_3-gas sampling artifacts of 3–4% for HNO_3 and 5–10% for HONO have been reported (Bai et al., 2003; Koutrakis et al., 1988). At temperatures >28 °C, HNO_3 readily absorbs and desorbs on surfaces due to interference of NO_2. Mean temperatures during the winter campaign NO_y 2001 were considerably lower (5 °C). The determination of N-species on uncoated quartz fibre filters can suffer from sampling artifacts like evaporation of semivolatile ammonium nitrate producing equimolar amounts of HNO_3 and NH_3 (Harrison and Pio, 1983) or retention of ambient HNO_3 on the filter (Appel et al., 1984). The use of denuder-filter systems is employed to prevent these artifacts. During both sampling campaigns pre-extracted quartz fibre filters were used.

Additional measurements of oxidised nitrogen on a daily basis were made by the University of Antwerp (Eyckmans et al., 2001) during the months of July, September and October 2000 (*summer/early autumn campaign NO_y 2000*). The sampling was made using a dual channel sequential fine particle sampler (URG 2000-01 K, United Research Glassware, NC, USA). Coarse particles above 10 μm diameter were separated at the air inlets. Air masses were drawn at a flow rate of 10 L min^{-1} through annular denuders in front of which a cyclone removed the particle fraction above 2.5 μm. For acid gases, a coating of methanol/ultrapure water (50/50), in which 1% glycerol and 1% Na_2CO_3 were dissolved, was applied to three concentric annular denuders. Teflon filter-holders placed behind the denuders were cleansed on a regular basis and loaded with Whatman filters (GF/F, 47 mm), and denuder sets were replaced every 4 days. Exposure duration and time of denuder change (midnight) were programmed through an electronic switching system.

Denuder coating was extracted with 2 × 5 mL Milli-Q (Millipore) water and analysed using ion chromatography (Dionex DX 120). The filters themselves were put in a plastic jar along with 10 mL Milli-Q water and extracted for 20 min in an ultrasonic bath. Afterwards, the solution was filtered through a 0.22 μm pore Millex filter (Millipore) and analysed using IC.

2.3.2. Throughfall water

Throughfall (TF) was sampled using 10 systematically distributed bulk collectors in the adjacent 0.25 ha large level II observation plot. They consisted of a polyethylene funnel (14 cm in diameter) placed at a standard height of 1 m, which was connected to a subterranean 2 L polyethylene bottle. A nylon mesh (1 mm) was placed in the funnel to avoid contamination by large particles. Samples from all collectors were pooled together for every sampling event, which took place 24 times a year. When insufficient rainfall was registered, sampling was postponed without replacing the sampling equipment. Bulk precipitation was collected using four bulk collectors placed at an adjacent pasture (about 250 m away from the tower location) with the same sampling frequency. Fractions of NH_4^+ and NO_3^- were analysed using ion chromatography (Dionex DX-100). Conversion factors from bulk deposition to wet deposition samplers were derived from a comparison exercise between bulk collectors and a wet-only sampler at another level II site near to Ghent (50°58′ N, 3°49′ E; see Staelens et al., 2005) and were estimated to be 85% and 79% for NH_4^+ and NO_3^-, respectively.

2.4. Calculation of nitrogen fluxes

Both gradient measurements and resistance models were applied to estimate ecosystem input. For the gases measured every half hour (NH_3 and NO_x), gradients from the 23 and 39 m interval (lower and upper profile height) were used to calculate fluxes applying the gradient method (Dyer and Hicks, 1970):

$$F = -K\frac{\partial c}{\partial z} \tag{1}$$

where F is the flux (in μg m^{-2} s^{-1}, defined positive upward), c is the concentration (μg m^{-3}), z is the height (in m) and K is the turbulent diffusivity (in m^2 s^{-1}), calculated as:

$$K = \frac{k(z-d)u_*}{\phi} \tag{2}$$

In this formula k (the von Karman constant) is 0.4, z is the geometric mean of the measurement heights (29.9 m), d is the zero plane displacement (=19.2 m) inferred from wind profile measurements, and u_* is the friction velocity determined as the (negative) square root of the kinematic momentum flux measured by eddy covariance. In order to account for stability effects, the universal flux–profile relationships for heat transfer (ϕ_h) were applied (Dyer and Hicks, 1970). Because the concentration measurements were made in the roughness sublayer, turbulent diffusivities estimated by Eq. (2) were corrected by a factor (α, here = 0.87) to allow for wake turbulence generated above the canopy (Bosveld, 1991):

$$\phi_h = \begin{cases} L \le 0 \ldots\ldots\ldots \alpha \times \left(1 - 16^{\frac{(z-d)}{L}}\right)^{-1/2} \\ L > 0 \ldots\ldots\ldots \alpha + 5^{\frac{(z-d)}{L}} \end{cases} \tag{3}$$

where L is the Monin–Obukhov length and $(z-d)/L$ the dimensionless stability height.

Data were screened to exclude measurement problems and conditions invalidating the use of flux–gradient theory. Friction velocities below 0.1 m s^{-1} were rejected because of probable invalid flux–profile relationships. A footprint analysis, carried out by Göckede et al. (2005) based upon source weight functions for all stratification regimes, revealed that the forest land use type contributed on average about 80% to each eddy covariance flux measurement at 41 m height. Analysis of horizontal structures in the raw turbulent data disclosed no disturbing influence of the surrounding landscape on the eddy covariance measurements. Therefore, no further rejection criteria were included to avoid potential perturbation effects due to limited fetch in NW direction. To avoid non-stationarity, data were excluded for which concentrations' changes lead to half hour changes in deposition velocity v_d exceeding 0.01 m s^{-1}, ($|z/c \times (dc/dt)| < 0.01$ m s^{-1}). Gradients were checked for systematic bias between the two heights during episodes of high turbulence ($u_* > 1.5$ m s^{-1}) and strong rain (>4 mm h^{-1}) for which gradients were expected to drop to zero. Unequal flow rates due to denuder malfunction or blocked sample lines (presence of soot or pollen) lead to biased gradients (time shift between denuder readings), which were omitted from the NH_3 data set. In order to reduce the relative errors, concentrations below 0.1 μg m^{-3} (in case of NH_3) or 1 ppb

(in case of NO_x) were excluded. Outliers in the data were removed, rejecting any deposition velocity exceeding $2/R_a$.

For NO and NO_2, flux divergence could possibly occur due to chemical reactions within the O_3/NO/NO_2 triad (Vilà-Guerau de Arellano and Duynkerke, 1992). Time scales for chemical reactions (τ_c) were compared with time scales of turbulent transfer (τ_t) in order to ensure that the constant flux assumption was not invalidated. The chemical reaction timescale τ_c was calculated according to Lenschow (1982), whereas τ_t was approximated according to Ammann (1999).

Fluxes of other gaseous compounds HONO and HNO_3, sampled on daily basis, were modelled. It was assumed that the gases were continuously deposited and no surface concentration existed:

$$F = -v_d(z)c(z) \tag{4}$$

where $v_d(z)$ is the deposition velocity at height z (m s^{-1}), and $c(z)$ is the concentration at reference height z.

Deposition velocity was inferred from measured meteorological variables using a resistance analogy in which v_d is calculated as the inverse of three resistances (Hicks et al., 1987):

$$v_d(z) = \frac{1}{R_a(z) + R_b + R_c} \tag{5}$$

where $R_a(z)$ is the aerodynamic resistance, R_b is the laminar sublayer resistance, and R_c is the canopy resistance.

Aerodynamic resistance $R_a(z)$ was calculated according to Garland (1978) and was the same for all gases:

$$R_a(z) = \frac{1}{ku_*}\left[\ln\left(\frac{z-d}{z_0}\right) - \psi_h\left(\frac{z-d}{L}\right) + \psi_h\left(\frac{z_0}{L}\right)\right] \tag{6}$$

where z_0 is the roughness length (1.4 m), and $\psi_h((z-d)/L)$ is the integrated stability correction for heat, estimated following Beljaars and Holtslag (1990).

R_b was species-dependent and estimated using semi-empirical relationships presented by Hicks et al. (1987) with Schmidt and Prandtl number corrections:

$$R_b = \frac{2}{ku_*}\left(\frac{Sc}{Pr}\right)^{2/3} \tag{7}$$

The canopy resistance (R_c) of gases consists of stomatal resistance (R_s), soil (R_{soil}) and in-canopy aerodynamic resistance (R_{inc}), together with cuticular resistance (R_w) acting in parallel:

$$R_c = \left[\frac{1}{R_s} + \frac{1}{R_{inc} + R_{soil}} + \frac{1}{R_w}\right]^{-1} \tag{8}$$

Terms in this equation were estimated for different gases using parameterisations mentioned in Erisman et al. (1994). Stomatal resistance (R_s) was calculated using the parameterisations by Wesely (1989) based on the method by Baldocchi et al. (1987). This parametrisation only needed data for global radiation and surface temperature and was corrected for the different diffusion coefficient of the gas involved compared to water vapour. Formulation for R_{inc} was modelled by Erisman et al. (1994). For HNO_3 it was assumed that it was deposited along the leaf surface with negligible R_w. Also for the soil a negligible R_{soil} was assumed. For HONO, data on R_w and R_{soil} were lacking and instead parameterisations for SO_2 deposition on wet surfaces were used because of a similar chemical propensity (Erisman et al., 1994).

Deposition velocity (v_d) for particles (pNH_4 and pNO_3) was calculated using the modified model of Slinn (1982):

$$v_d = v_g + \left[R_a(50) + v_{ds}^{-1}\right]^{-1} \tag{9}$$

where v_g is the gravitational settling velocity of particles and v_{ds} is the surface deposition velocity, and $R_a(50)$ is the aerodynamic resistance at 50 m height. Due to only small-sized particles ($v_g \approx 0$) having been collected, Eq. (9) was reduced to a turbulent contribution and a surface deposition velocity. Particle deposition was modelled following the assumption of similarity to momentum deposition (Chamberlain, 1966; Slinn, 1982):

$$v_{ds} = E\frac{u_*^2}{u_h} \tag{10}$$

where u_* is the friction velocity, u_h is wind speed at the top of the canopy, and E is the total collection efficiency with which particles are captured by the canopy. The collection efficiency for pNO_3 and pNH_4 was calculated using parameterisations presented by Ruijgrok et al. (1997) made for coniferous forest. The relationships used for calculating E took into account different responses among the depositing components for conditions of u_*, leaf wetness (no particle rebound for wet surface) and ambient relative humidity (hygroscopic growth).

2.5. Data handling and statistics

Given the problems in handling the AMANDA analyser in harsh winter conditions and the removal of biased gradients, the data coverage was 33% during the operation period (June 1999–November 2001). In order to obtain complete budgets for NH_3, gap filling was performed using a single-hidden-layer feed-forward neural network (Saxén and Saxén, 1995). Given the importance of canopy wetness in ammonia deposition patterns (Neirynck et al., 2005), the half hourly data set was subdivided into different canopy wetness categories: rainy conditions (rainfall measured by pluviometer) and non-rainy conditions (no rainfall measured by pluviometer). The latter were further subdivided into three classes depending on the grid wetness of the leaf wetness sensor: 0% (dry); 0% < wetness < 100% (wet); 100% (saturated). The neural network (NN) training and subsequent gap filling was carried out separately for each wetness category. The complete data set from each category was randomly divided in two even-sized sets. Neural networks were trained with relevant variables (such as NH_3, u_*, $(z-d)/L$, temperature, …) from one data set (training data set), evaluated with the other (test data set) and then used to fill missing values of NH_3 flux. When no NH_3 measurements from the monitor (single height) were available, daily measurements from honeycomb denuders (NH_x campaign) were used as input to fill missing fluxes. Networks were also trained without information regarding NH_3 or molar NH_3/SO_2 ratio. When data on atmospheric turbulence were lacking, no NN were trained and no gap filling was done. Fluxes for which no robust calculation was possible because concentrations fell below the detection limit ($c < 0.1$ μg m^{-3}) or low turbulence ($u_* < 0.1$ m s^{-1}) prevailed, were set to zero given the expectation of negligible fluxes.

Given the seasonal differences in concentrations and fluxes, data set was subdivided into a summer season (April–September) and a winter period (October–March).

3. Results

3.1. Composition and variability of nitrogen in atmosphere

Nitrogen dioxide (NO_2) was the prevailing nitrogen compound in the lower troposphere at the site (Table 1). Its average concentration of 8.7 μg N m^{-3} was two to three times higher compared to nitric oxide (NO) and ammonia (NH_3). Nitrogen oxides were higher in concentration than NH_3 during the winter (Fig. 2A). During summer, levels of NH_3 strongly increased and even approached the declining NO_2 levels (Fig. 2B).

Nitrogen oxides exhibited pronounced diurnal patterns that featured a strong morning peak for NO (Fig. 2A and B). The NO peak occurred earlier in the morning during the summer and was lower in magnitude. Peaking occurred approximately 1 h after sunrise time. The diurnal pattern of NH_3 was flattened during the winter period but more susceptible to atmospheric mixture during the summer.

Table 1
Statistical parameters of nitrogen compounds (NH_3, NO and NO_2, pNH_4, HONO, HNO_3, pNO_3) measured at 0.5 h or 24 h time steps above the canopy for measurements conducted between July 1999 and November 2001 (in $\mu g\ N\ m^{-3}$)

Compound	Period	n	Arith av	σ	median	min	max	Geom. Av	Geom. σ
0.5 h sampling									
NH_3	Jul 99–Nov 01	15,047	3.0	5.6	1.3	0.0	102.5	1.2	3.5
NO	Jul 99–Nov 01	39,226	3.9	12.5	0.0	0.0	291.7	1.3	2.0
NO_2	Jul 99–Nov 01	39,228	8.7	6.2	7.5	0.0	55.4	6.9	1.3
24 h sampling									
pNH_4	Sep 99–Jun 00	225	2.0	1.6	1.5	0.2	8.8	1.5	1.7
NH_3	Sep 99–Oct 00	299	2.4	2.6	1.5	0.1	17.5	1.6	1.9
HONO	Jul, Sep, Oct 00	72	0.5	0.4	0.4	0.0	1.4	0.4	0.8
	Jan, Feb, Mar 01	85	0.5	0.5	0.4	0.0	2.6	0.4	0.7
HNO_3	Jul, Sep, Oct 00	72	0.15	0.15	0.12	0.00	1.13	0.13	0.4
	Jan, Feb, Mar 01	85	0.05	0.06	0.02	0.02	0.42	0.03	0.5
pNO_3	Jul, Sep, Oct 00	67	0.5	0.3	0.4	0.0	1.8	0.4	0.5
	Jan, Feb, Mar 01	85	1.2	0.9	1.1	0.0	3.8	0.9	0.5

Particles of NH_4, which were measured during eight non-consecutive months on a daily basis (Table 1), were lower in arithmetic mean concentration than NH_3 captured by denuders but median and geometric mean were similar to those of NH_3. The two compounds were significantly correlated ($R^2 = 0.41$, $n = 226$) and exhibited highest levels during summer time. Particles of NO_3 were particularly abundant during the winter campaign, in contrast to HNO_3, which only appeared in substantial quantities during summer/early autumn. During both campaigns, levels of HONO were more elevated than those of HNO_3.

Levels of measured nitrogen compounds were strongly dependent on wind direction (Fig. 3A and B), determined by nearby emission sources. High levels of NO, NO_2 and HONO originated from the W-ESE sector. Nitric oxide reached its highest levels in the SSW-S sector, whereas HONO peaked in the ESE or S sector. Nitrous acid was correlated with NO and NO_2 ($R^2 = 0.42$, $n = 127$). Nitric acid (wind sector dependence not shown) was uncorrelated to these possible precursors and other nitrogen compounds. North-easterly winds brought NH_x-enriched air masses to the site, although pNH_4 seemed to be associated with a larger range of wind directions than NH_3. Nitrate particles, possibly pertaining to ammonium nitrate-bearing particles, peaked when winds blew from the ENE sector.

3.2. Atmospheric nitrogen fluxes

3.2.1. Characteristics of dry deposition fluxes

After applying the above-mentioned rejection criteria, 8824 half hourly flux values were retained with an average net NH_3 flux of $-75 \pm 145\ ng\ N\ m^{-2}\ s^{-1}$ with a corresponding v_d of $3.0 \pm 4.6\ cm\ s^{-1}$ (Neirynck et al., 2005; Table 2). Net NH_3 flux measured during the summer period was three times higher compared to winter period flux. This was rather due to lower NH_3 levels during winter since average v_d differed only slightly across season (Table 3). The small differences in v_d could be explained by the fact that daily atmospheric resistances ($R_a + R_b$) and canopy resistance (R_c) varied only slightly among season. At nighttime, however, summer $R_a + R_b$ and R_c were almost two times higher compared to winter season values which resulted in a lower nighttime summer v_d of $1.7\ cm\ s^{-1}$.

Neural networks (NN) were trained with measured NH_3 flux data and used to predict missing values for different

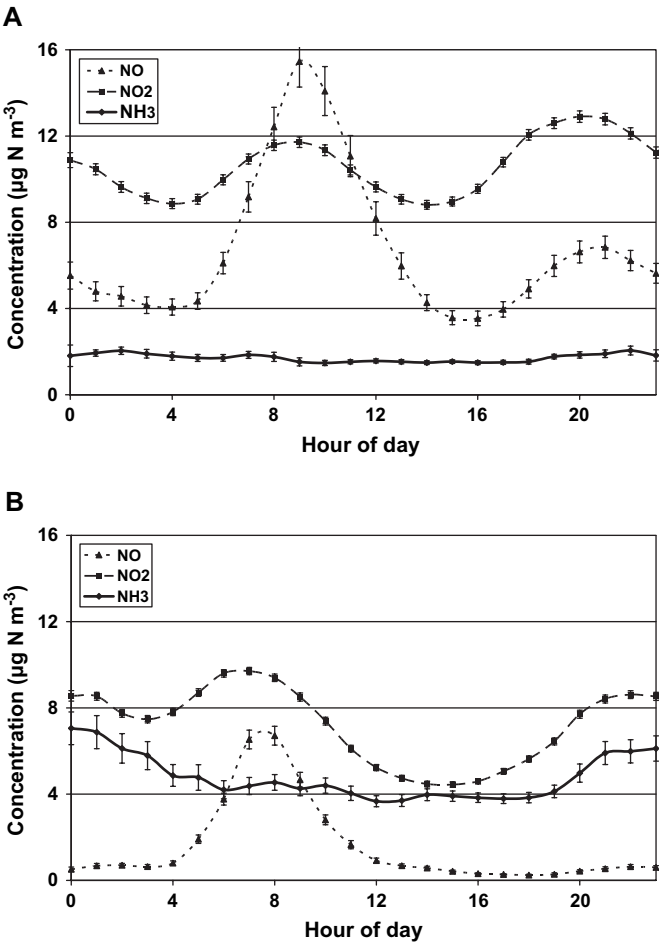

Fig. 2. Averaged diurnal course of NO, NO_2 and NH_3 concentrations (standard error shown by bars) for winter (A) and summer (B) at a height of 40 m.

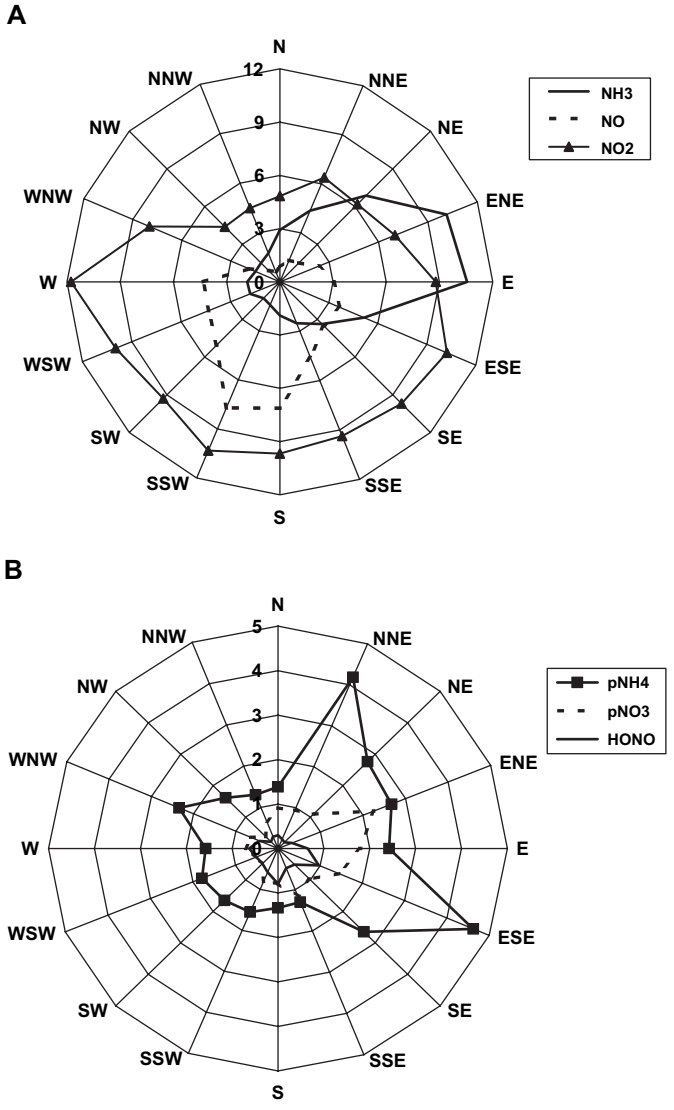

Fig. 3. Wind sector dependencies of average concentration of NH_3, NO, NO_2 (A) and HONO, pNO_3 and pNH_4 (B) for the Brasschaat forest site during the period June 1999–November 2001 (in $\mu g\,N\,m^{-3}$) (HNO_3 is not shown because of low concentrations).

canopy wetness categories (definition see above). Explanatory variables in the training set were found to be u_*, $(z-d)/L$, NH_3, NH_3/SO_2, temperature (T), relative humidity (RH), photosynthetic photon flux density (PPFD) and wind direction. When trained NN performance was evaluated with test data sets (Table 4), best agreement between measurements and NN values was obtained when canopy was dry ($R^2 = 0.59$; Fig. 4). Predictions made by NN were worst during rainy conditions; a departure >25% from measured mean and median flux was found and R^2 was only 30%.

Gap filling of NH_3 fluxes assuming null NH_3 fluxes for low turbulence or low concentration data resulted in an increase of data coverage from 20% ($n = 8824$) to 33% ($n = 14{,}560$). When also NN predicted data were used, data coverage rose to 87% ($n = 37{,}123$) (Fig. 5). This was especially helpful for achieving a better flux estimate for winter conditions during which measuring equipment was difficult to handle or not operational which was the case in winter 2000–2001. An average net NH_3 flux of $-64 \pm 120\ ng\,N\,m^{-2}\,s^{-1}$ was obtained for the entire measuring period (Table 2). Same conclusions drawn for the measured fluxes applied also for the completed flux data set but fluxes were about 10–15% lower compared to the measured fluxes and the average v_d decreased to $2.8 \pm 5.1\ cm\,s^{-1}$. Measured fluxes and fluxes including gap filled data featured a different diurnal pattern during both winter and summer (Fig. 6A). Measured fluxes were always higher compared to the gap filled data set except at noon, during which fluxes dropped as a result of increased emission or reduced uptake at the canopy.

For NO_x, the presence of flux divergence above the canopy was tested before the gradient method could be applied. An analysis of the timescale ratios τ_c/τ_t revealed that for 87% of the observations, turbulence time scales (τ_t) were more than one order of magnitude smaller than chemical reaction time scales (τ_c). The observations during which response time of diffusive transfer was in the same order of magnitude as chemical reactions coincided with calm, stable (nighttime) conditions. These observations ($u_* < 0.1\ m\,s^{-1}$) were, however, rejected from the data set because fluxes were uncertain to calculate. Slow chemistry between the reference height and the surface could therefore be assumed and a direct flux calculation of the $NO/NO_2/O_3$ triad by the gradient method was

Table 2
Total and seasonal averages and standard deviations of flux characteristics of NH_3 (measured and including gap filled data) and NO_x measured on a half hourly basis during the period July 1999–November 2001

		Method	n	F ($ng\,N\,m^{-2}\,s^{-1}$)	σF ($ng\,N\,m^{-2}\,s^{-1}$)	v_d ($cm\,s^{-1}$)	σv_d ($cm\,s^{-1}$)
NH_3	Total	Gradient meas.	8824	−75	145	3.0	4.6
	Winter[b]		3729	−36	69	3.2	4.8
	Summer		5095	−104	176	2.8	4.5
NH_3	Total	Gradient + gap filling[a]	37,123	−64	120	2.8	5.1
	Winter		15,480	−31	56	2.9	5.1
	Summer		18,077	−93	150	2.7	5.0
NO_x	Total	Gradient meas.	26,603	+8.5	259	−0.04	3.1
	Winter		11,905	+9.4	282	0.00	2.8
	Summer		14,698	+7.8	239	−0.07	3.4

[a] Including gap filled data obtained by neural network and previously rejected data for which NH_3 levels <0.1 $\mu g\,m^{-3}$ and $u_* < 0.1\ m\,s^{-1}$ which were assumed to be zero.

[b] Winter period: October–March; Summer: April–September.

Table 3
Characteristics of NH_3 flux measurements during summer and winter period

	Summer			Winter		
	Daytime	Nighttime	Whole day	Daytime	Nighttime	Whole day
n	3238	1857	5095	1496	2233	3729
NH_3 ($\mu g\,N\,m^{-3}$)	4.0	4.3	4.1	1.5	1.6	1.6
Flux ($ng\,N\,m^{-2}\,s^{-1}$)	−132	−54	−104	−40	−34	−36
v_d ($cm\,s^{-1}$)	3.4	1.7	2.8	3.6	3.0	3.2
$R_a + R_b$ ($s\,m^{-1}$)	23	53	34	23	34	30
R_c50 ($s\,m^{-1}$)[a]	9.1	35.3	15.9	13.1	19.8	17.4

[a] R_c50, median from $1/v_d - R_a - R_b$ after omitting upward fluxes.

tenable. It was decided take to NO_x ($NO + NO_2$) gradients to calculate the total NO_x flux because it was a more robust measurement based estimate of NO_x exchange (sum stays conserved) and less NO_x fluxes were omitted because NO_x levels were seldom below the detection limit (1 ppb) compared to a separate analysis.

Net NO_x flux was upward ($8.5\,ng\,N\,m^{-2}\,s^{-1}$) with a net-emission velocity v_d of $-0.04\,cm\,s^{-1}$ (Table 2). No marked differences in flux magnitude between summer and winter period could be detected. Highest emissions up to $40\,ng\,N\,m^{-2}\,s^{-1}$ were observed in the morning (Fig. 6B) but NO_x exchange tended to net-deposition at noon.

Other N compounds, measured every 24 h, contributed significantly to the dry flux of nitrogen (Table 5). The flux of pNH_4 amounted to $-20\,ng\,N\,m^{-2}\,s^{-1}$, which comprised about 30% of the net NH_3 flux. The dry deposition flux of the remaining oxidised nitrogen compounds amounted to −20 and $-27\,ng\,N\,m^{-2}\,s^{-1}$ for the summer and winter campaigns, respectively (Table 5). The flux of HONO amounted to about $-9\,ng\,N\,m^{-2}\,s^{-1}$, irrespective of season. Contributions of pNO_3 and HNO_3 presented important seasonal changes. During the winter campaign deposition of pNO_3 was three times higher than the summer flux because of both higher v_d (due to higher relative humidity and leaf wetness during winter) and measured concentrations. The opposite was the case for HNO_3, the flux being more important during the summer period when its concentration was substantially higher.

3.2.2. Total nitrogen deposition versus throughfall

Total nitrogen deposition (TD), calculated as the sum of wet deposition (WD) and dry deposition (DD), was estimated at $-48\,kg\,N\,ha^{-1}\,yr^{-1}$ (Table 6). Wet deposition of NH_4^+ and NO_3^-, derived from bulk deposition, amounted to −17.5 kg and comprised 36% of TD. Wet deposition consisted mainly

Table 4
Comparison of measured fluxes from test files with their output results from trained neural networks (NN) for different canopy wetness categories (in $ng\,N\,m^{-2}\,s^{-1}$)

Canopy wetness	n	Mean fluxes		Median fluxes		Performance
		Meas.	NN	Meas.	NN	R^2
Dry	1547	111	108	34	38	0.59
Wet	622	54	63	25	25	0.40
Saturated	1135	40	42	14	15	0.54
Rainy	198	38	48	23	18	0.28

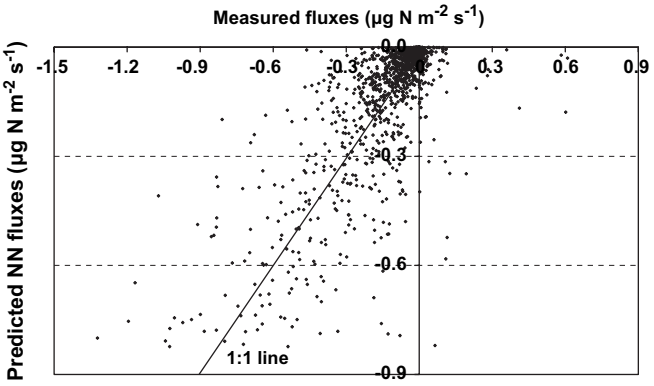

Fig. 4. Measured fluxes from test data set versus fluxes predicted by NN for a dry canopy (in $\mu g\,N\,m^{-2}\,s^{-1}$).

of NH_4^+ (69%) and was slightly higher during the summer period. Dry deposition was estimated at $-30.7\,kg\,N\,ha^{-1}\,yr^{-1}$ (64% of TD) and consisted mainly of NH_x ($-26\,kg\,N\,ha^{-1}\,yr^{-1}$). Dry deposition of NH_3 contributed for 41% and 64% to TD and DD, respectively, and its share was even higher during the summer period when its amount raised to $-29.3\,kg\,ha^{-1}$ on annual basis. Due to its preponderance in WD and DD, NH_x contributed for 79% to TD. Share of NO_y compounds in DD was minor compared to NH_x and was of similar magnitude as $WD_{NO_3^-}$.

Throughfall (TF) of NH_4^+ amounted to $-23\,kg\,N\,ha^{-1}\,yr^{-1}$ and was 50% higher during the summer period (Table 6). This was in line with higher estimated DD of NH_3 during the summer period. Total deposition of NH_x exceeded $TF_{NH_4^+}$ with $-15\,kg\,N\,ha^{-1}\,yr^{-1}$ (or 31% of TD) indicating substantial uptake of NH_x by the canopy. Canopy uptake of NH_x was higher during the summer period with canopy uptake rates being more than twice as large compared to winter period.

Good agreement was observed when the sum of WD of NH_4^+ and DD fluxes of NH_3, which were accumulated − and partly washed off − during the 2–3 weeks exposure of the TF collectors, were regressed against the TF amounts captured during the same sampling interval (Fig. 7). Throughfall amounts of NH_4^+ (expressed per ha and per sampling event), which varied between 0.1 and $3.6\,kg\,N\,ha^{-1}\,sampling^{-1}$, were positively correlated ($n = 42$; $R^2 = 0.70$) with the sums of estimated DD of NH_3 and measured $WD_{NH_4^+}$ captured within the same sampling interval. The slope of the regression line exceeded unity confirming presence of canopy uptake.

Throughfall of NO_3^- amounted to $-10.1\,kg\,N\,ha^{-1}\,yr^{-1}$ and was also 50% higher during the summer period. This was, however, not in agreement with DD of NO_y the global estimate of which was more elevated during the winter. Throughfall of NO_3^- did not differ from TD of NO_y indicating lacking canopy uptake.

4. Discussion

4.1. Concentrations

Analysis of the nitrogen levels at a suburban forest near Antwerp revealed the presence of high gaseous NO_x. Nitrogen

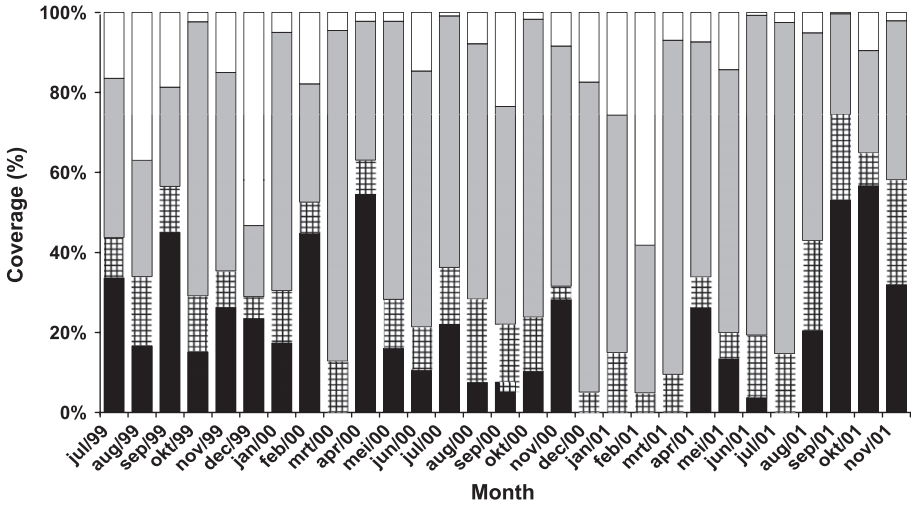

Fig. 5. Monthly data coverage over July 1999–November 2001 including: (1) data measured (in black); (2) data assumed zero (crossed); (3) data NN filled (in grey); (4) data not filled (in white).

dioxide (NO_2) was found to be the most important N compound, followed by NO and NH_3. High pollution levels of NO and NO_2 in southwesterly winds at the measuring site were due to vehicle emissions or other (industrial, suburban) combustion sources. The correlation between HONO and NO/NO_2 and their respective wind dependencies indicated a similar emission source, or its formation from these precursors. The ratio of $HONO/NO_2$ amounted to 8%, which is much higher than the ratio measured by nearby combustion sources (<1%) (Kurtenbach et al., 2001). On site formation of HONO from NO_2, which could occur through reaction with aerosols (Reisinger, 2000), water vapour (Harrison et al., 1996) or light absorbing organic substances (Kleffmann et al., 2003), could therefore not be precluded. Although HONO is strongly susceptible to photolysis during the daytime, its levels were higher than for HNO_3. The latter compound was found to be low in concentration, which was possibly due to the generally high ammonia background concentrations in Flanders.

High levels of reduced nitrogen originating from agricultural activities situated in the eastern sector contributed significantly to the nitrogen pollution climate. The presence of NH_3 also led to the advection of significant amounts of NH_4- and NO_3-bearing aerosols, converted from NH_3 during transport to the site. The variable distance in location of the emission sources (less than 5 km to more than 10 km) and differences in the vegetation composition in the upwind direction might be the reason for the observed variability in the NH_3/NH_4 ratio of the air masses reaching the tower site for a given wind sector.

4.2. Fluxes

Dry deposition fluxes of nitrogen were dominated by NH_3 for which the flux was estimated at -64 ng N m^{-2} s^{-1}. Fluxes of a similar magnitude (55–85 ng N m^{-2} s^{-1}) were measured in the Netherlands above a Douglas forest (Wyers et al., 1992; Wyers and Erisman, 1998). In order to complete the annual NH_3 budget, gaps in data set were filled by estimates obtained by neural networks. Neural networks performed the best when the canopy was dry, which was the predominant canopy wetness category (44% of all cases) at our site (Neirynck et al., 2005). During these conditions more turbulence is generated and fluxes can be measured (and estimated) more precisely. During rainy conditions, deviations from measured fluxes

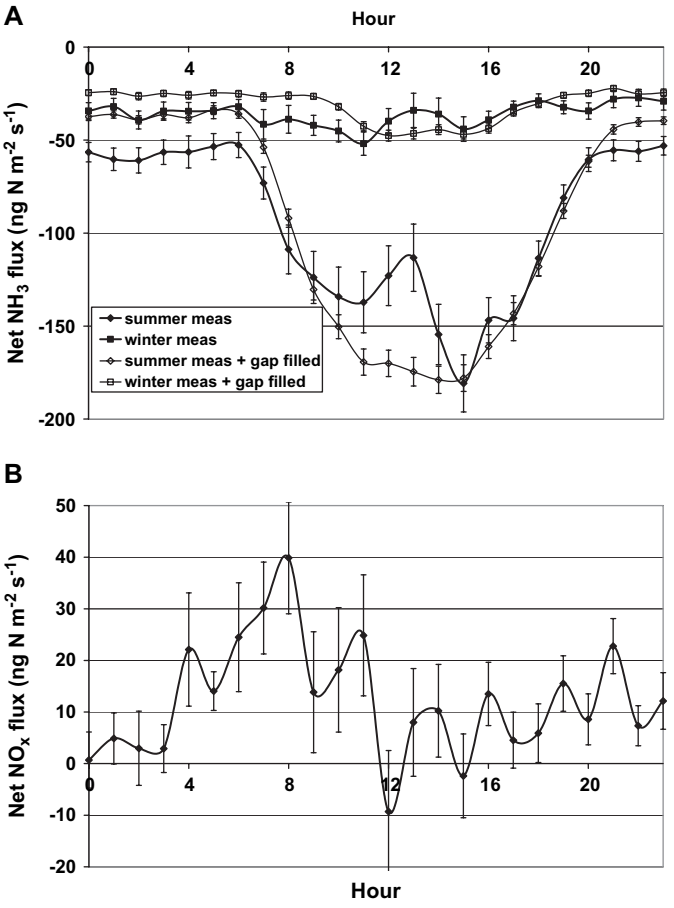

Fig. 6. Averaged diurnal course of measured ($n = 8824$) and gap filled ($n = 37{,}123$) NH_3 fluxes (A) and measured ($n = 26{,}603$) NO_x fluxes (B) (in ng N m^{-2} s^{-1}). Standard errors are shown by bars.

Table 5
Averaged flux characteristics for N compounds measured on daily basis

	Period	n	F (ng N m^{-2} s^{-1})[a]	v_d (cm s^{-1})
pNH_4	Sep 99 till Jun 00	9309	−20	1.2
pNO_3	Jun/Sep/Oct 00	2360	−5.0	1.2
	Jan/Feb/Mar 01	2356	−16	1.5
HNO_3	Jun/Sep/Oct 00	3317	−6.4	4.2
	Jan/Feb/Mar 01	3040	−2.0	4.5
HONO	Jun/Sep/Oct 00	3317	−8.6	2.4
	Jan/Feb/Mar 01	3040	−9.2	2.0

[a] Fluxes were obtained by multiplying the half hourly-modelled v_d with daily measured concentrations.

were the worst. In these conditions, which represent 9% of the data set, fluxes are hard to measure and so were simulations.

The flux of NH_3 exhibited a strong seasonal variability, with summer deposition three times higher compared to winter conditions (Table 2, Fig. 6A). This is due to higher NH_3 levels as a consequence of higher temperatures during summer and manure spreading prohibition during winter time. Deposition velocities did not vary substantially across the season although a decreased v_d was noticed during summer at night (Table 3).

When NO_x fluxes were calculated with the gradient method, the net flux appeared to be upward (8.5 ng N m^{-2} s^{-1}), with the highest net-emission of NO_x measured in the morning (40 ng N m^{-2} s^{-1}). Above-canopy fluxes calculated using the gradient analysis incorporate, besides deposition from ambient NO_x, also emitted NO_x fluxes from the canopy surface. We speculate that NO_x emissions originated from soil-emitted NO, typically occurring in nitrogen-impacted forests (http://195.127.136.75/nofretete/). Emitted NO was probably stored in the trunk or canopy space during stable events, as indicated by the distinct morning peak (Fig. 2). Upon the initiation of turbulence, the stored NO below the canopy underlies rapid oxidation to NO_2 in the presence of ozone entrained from above (Dorsey et al., 2004; Duyzer et al., 2004). The surplus of NO_2 formed above the canopy led to negative gradients and upward fluxes, especially during the morning. Later at noon, the net NO_x flux tended to be directed towards the canopy, possibly as result of increased deposition of airborne NO_2. Such a dual pattern of counteracting fluxes was also observed in a Douglas fir forest in the Netherlands (Duyzer et al., 2004).

Fluxes of pNH_4 and pNO_3 have been estimated using parameterisations for a Douglas fir stand in the Netherlands. The application of these models was justified since deposition velocities of small aerosols were found to be underestimated for very rough surfaces (Gallagher et al., 1997; Ruijgrok et al., 1997). Modelled v_d of pNH_4 (1.2 cm s^{-1}) were similar to those measured for ammonium(bi)sulphate (MMD 0.8 μm) by Wyers et al. (1995) over the forest site in the Netherlands, with average values of 1.2–1.5 cm s^{-1}. They were, however, higher than experimentally derived v_d of pNH_4 for ammonium sulphate particles in Hungary (0.8 cm s^{-1}) (Horváth, 2003) or when obtained with wash-off methods (Marques et al., 2001 and literature mentioned therein).

Table 6
Wet deposition (WD) and dry deposition (DD) of NH_x and NO_y versus annual throughfall (TF) of NH_4^+ and NO_3^- (in kg N ha^{-1} yr^{-1})

		NH_x					NO_y				$NH_x + NO_y$			
		Summer	Winter	Total	% TD		Summer	Winter	Total	%TD	Summer	Winter	Tot	%TD
WD	NH_4^+	−13.5	−10.5	−12.0	*25%*	NO_3^-	−5.7	−5.2	−5.5	*11%*	−19.3	−15.7	−17.5	*36%*
DD	NH_3	−29.3	−9.8	−19.6	*41%*	NO_x	2.5	3.0	2.7	*−6%*				
	pNH_4	−6.2	−6.8	−6.5	*13%*	HONO	−2.7	−2.9	−2.8	*6%*				
						HNO_3	−2.0	−0.6	−1.3	*3%*				
						pNO_3	−1.6	−5.0	−3.3	*7%*				
	Sum	−35.5	−16.5	−26.0	*54%*	Sum	−3.8	−5.6	−4.7	*10%*	−39.3	−22.1	−30.7	*64%*
TD	NH_x	−49.1	−27.0	−38.0	*79%*	NO_y	−9.6	−10.8	−10.2	*21%*	−58.6	−37.8	−48.2	*100%*
TF	NH_4^+	−27.9	−18.1	−23.0	*48%*	NO_3^-	−12.1	−8.1	−10.1	*21%*	−40.0	−26.1	−33.1	*69%*
Canopy uptake[a]		−21.1	−8.9	−15.0	*31%*		2.5	−2.7	−0.1	*0%*	−18.6	−11.7	−15.2	*31%*

Percent contribution of each compound in total nitrogen deposition is given in additional column.
[a] Canopy uptake is calculated as TD − TF.

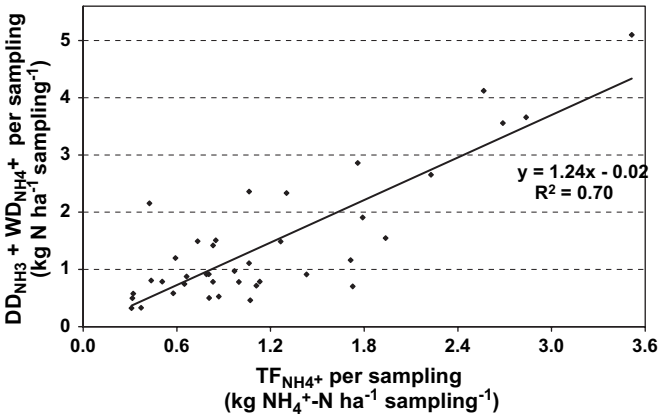

Fig. 7. Sum of estimated dry deposition of NH_3 (DD_{NH_3}) and measured wet deposition of NH_4^+ ($WD_{NH_4^+}$) captured per sampling interval of 2–3 weeks, plotted against measured throughfall NH_4^+ ($TF_{NH_4^+}$) measured during the same sampling interval.

Modelled v_d for HNO_3 were in line with those determined for deciduous forest (Meyers et al., 1989; Pryor et al., 2002) but lower than for coniferous forests (Pryor and Klemm, 2004; Sievering et al., 2001). Fluxes and concentrations differed strongly between the two measuring seasons, which might reflect a shift in the thermodynamic equilibrium between gaseous HNO_3 and pNO_3. According to Seinfeld and Pandis (1998), higher temperatures (which we encountered during the summer/autumn campaign) favoured shifts in concentrations of HNO_3 relative to pNO_3. This led to opposing seasonal deposition patterns of both compounds above a pine forest in Germany (Dämmgen and Zimmerling, 2002).

Deposition velocities of HONO were estimated to be lower than those for HNO_3, but higher concentrations compensated, resulting in fluxes of a similar magnitude. The mean v_d of 2–2.4 cm s^{-1} was similar to modelled values of Dämmgen and Zimmerling (2002) but higher than the modelled mean of 1.3 cm s^{-1} for a spruce forest in Germany (Zimmermann et al., 2006).

4.3. Comparison of total deposition with throughfall data

When all compounds were added up, a TD of −48 kg N ha^{-1} yr^{-1} was obtained, with NH_x being the main contributor to DD and WD. This estimate largely exceeded the nitrogen TF deposition of −33 kg N ha^{-1} yr^{-1}, which is in line with other nitrogen flux studies on nitrogen-impacted forest sites (Dämmgen and Zimmerling, 2002; Marques et al., 2001; Schmitt et al., 2005). Although this discrepancy could partly be associated with general difficulties in relating throughfall measurements to the footprint of the measuring site, canopy uptake of N could not longer be ignored.

Uptake of N by the canopy is primarily the result of ion uptake by foliar and branch tissues or active uptake by canopy lichens and micro organisms (Lovett and Lindberg, 1993). Canopy budget models (Ulrich, 1983) are often applied to correct TF for possible canopy uptake of NH_4^+ exchanged for base cations. These models are quite senseless at our site since possibilities for base cation exchange were negligible (Neirynck et al., 2004). Ferm and Hultberg (1999) suggested that dry-deposited NH_x, consumed by the canopy, could later reappear as organic N in the TF samplers. Recent measurements of organic N showed at our site that DON constituted a substantial fraction of the total nitrogen concentration (10–15% of N_{tot}). Throughfall enrichment by organic N originating from deposited inorganic N, utilised at the canopy level, could therefore not be excluded.

4.4. Possible uncertainties in nitrogen fluxes and nitrogen budget

Part of the flux estimates relies on resistance models, whose uncertainty is difficult to quantify. The advantages of such models include simplicity, and widespread use allowing for comparison with other sites. In the case of particle deposition, the momentum analogy employed (Eq. (10)) belies differences in canopy sink mechanisms for momentum and particles: inertial impaction of particles is most efficient for the smallest obstacles, which in the canopy would be needles (Langmuir, 1961) but obstacle size has not been taken into account in the collection efficiency E. Momentum, on the other hand, is more efficiently absorbed by form (pressure) drag over more bulky protrusions (Thom, 1975).

The fact that only small-size particles ($PM_{2.5}$) were collected and analysed in our measuring programme might cast further doubt on our particle deposition results. This might constitute an underestimate, especially for pNO_3, which include particles over a wide size range (Lovett and Lindberg, 1986). At coastal areas, reactions between marine dominated and polluted air masses may shift pNO_3 onto the coarse mode (Yeatman et al., 2001). Schaap et al. (2002) though, provided strong arguments that nitrate concentrations over continental Western Europe were predominantly present in the fine aerosol fraction.

In this study, nitrogen compounds were measured at two different time scales, and daily sampling of some nitrogen compounds was required to ensure high analytical precision. The short-term variation was therefore not completely captured and, depending on the relation between concentration and deposition velocity, a non-systematic bias could be expected (Andersen and Hovmand, 1999).

The fact that fluxes are assumed to be proportional to concentrations when using the resistance approach gives rise to further criticism of results. In case of HONO and HNO_3, it was assumed that there was no substantial surface concentration and no emission could occur. Consequently, v_d and R_c are independent of measured concentration and fluxes can simply be derived from v_d. For some gases, however, a surface concentration or compensation point must be considered, because of limited uptake capacity in certain conditions and occurrence of emissions. In our measuring conditions, v_d of NH_3 was found to decrease with increasing ammonia levels because of saturation effects (Neirynck et al., 2005). Non-linearity between flux and concentration was also noticed by Horii et al. (2004) for NO_2 and Tarnay et al. (2002) for HNO_3.

The bidirectional nature of some species (NH_3, NO_x, HONO) obviously thwarts the unambiguous completion of the nitrogen budget at our site. At present, we can only conjecture what the sources and sinks for these species might be and in-depth analysis is required. In case of NH_3, emission events were observed and both stomata as saturated water films were surmised to be the cause of these emissions (Neirynck et al., 2005). Bidirectional models should therefore be preferred for gap filling procedures of NH_3 fluxes instead of neural networks although complex compensation point models require much information about stomatal compensation points along with acidity and thickness of water films covering the leaves (Sutton et al., 1998). Also more information is required about the chemical behaviour of HONO, which was assumed to act similarly to SO_2. We presume that the estimate of the HONO flux is associated with large uncertainties since a proportion of HONO measured above the canopy might be released from the forest floor after reduction of NO_2 and also subjected to emission (Kleffmann et al., 2003). Inclusion of downward HONO flux in the nitrogen budget may therefore overestimate the real N input. Also sources and sinks for NO_x have not yet been clearly identified at our site. More information is needed about the impact of possible NO soil emission on the budget of NO_y. Part of the NO converted to NO_2 can also be recovered by the canopy through stomatal uptake (Duyzer et al., 2004), further entangling the nitrogen budget.

5. Conclusions

Nitrogen dioxide was found to be the main nitrogen compound measured above this nitrogen-saturated suburban forest. It was shown that the canopy surface acted as a source for NO_x with highest emissions in the morning.

Reduced nitrogen was found to be the main contributor to dry and wet deposition. Total deposition at our site was ruled predominantly by dry deposition, given the neighbouring presence of agricultural, combustion and industrial sources. Sites located further away from these sources will be less exposed because dry-deposited substances are depleted from the air travelling downwind (Lovett, 1994). Such environmental conditions are, however, rarely met in a densely populated and industrially developed region such as Flanders.

Total nitrogen exceeded throughfall inputs, which was in line with other nitrogen flux studies at nitrogen-impacted sites. Although modelled dry deposition in these studies must sometimes be regarded as an upper limit, throughfall inputs systematically underestimate total inputs and hence, presence of substantial canopy sinks can therefore not be ignored (Lovett and Lindberg, 1993).

Acknowledgements

The purchase of the AMANDA monitor, the employment of our gratefully acknowledged expert Yves Buidin by our Institute, and the denuder measurements conducted by VITO were supported by VLINA (Flemish Impulse Program on Nature Development). This project was performed under the authority of the Flemish Minister of Environment and was instigated by Stijn Overloop, Peter Roskams and Jos van Slycken. The Flemish Environment Agency (VMM) financed additional measurements of NO_y by the Department of Chemistry from the University of Antwerp (Prof. R. Van Grieken). Sampling of throughfall and bulk deposition was carried out within the framework of the UN/ECE intensive monitoring of forest ecosystems. ASK is a *Ramon y Cajal* fellow, supported by the Spanish Ministry of Science and Technology, National Scientific Research Plan for Technological Development and Innovation.

References

Adams, P.J., Seinfeld, J.H., Koch, D., Mickley, L., Jacob, D., 2001. General circulation model assessment of direct radiative forcing by the sulfate–nitrate–ammonium–water inorganic aerosol system. Journal of Geophysical Research 106, 1097–1111.

Ammann, C., 1999. On the Applicability of Relaxed Eddy Accumulation and Common Methods for Measuring Trace Gas Fluxes. Zürcher Geographische Schriften 73. ETH, Zürich.

Andersen, H.V., Hovmand, M.F., 1999. Review of dry deposition measurements of ammonia and nitric acid to forest. Forest Ecology and Management 114, 5–18.

Appel, B.R., Tokiwa, Y., Haik, M., Kothny, E.L., 1984. Artifact particulate sulfate and nitrate formation on filter media. Atmospheric Environment 18, 409–416.

Bai, H., Lu, C., Chang, K.-F., Fang, G.-C., 2003. Sources of sampling error for field measurement of nitric acid gas by a denuder system. Atmospheric Environment 37, 941–947.

Baldocchi, D.D., Hicks, B.B., Camara, P., 1987. A canopy stomatal resistance model for gaseous deposition to vegetated surfaces. Atmospheric Environment 21, 91–101.

Barthelmie, R.J., Pryor, S.C., 1998. Implications of ammonia emissions for fine aerosol formation and visibility impairment – a case study from the lower Fraser Valley, British Columbia. Atmospheric Environment 32, 345–352.

Beljaars, A.C.L., Holtslag, A.A.M., 1990. Description of a software library for the calculation of surface fluxes. Environmental Software 5, 60–68.

Berghmans, P., Daems, J., Bleux, N., Swaans, W., June 2001. Measurements of Ammonium Aerosol. Measurements of Oxidised Nitrogen. 2001/MIM/R90. VITO, 35 pp. (in Dutch).

Bosveld, F.C., 1991. Turbulent Exchange Coefficients over a Douglas Fir Forest. Final report Dutch Priority Programme on Acidification, Project 190.1. Royal Netherlands Meteorological Institute (KNMI), De Bilt.

Butler, T.J., Likens, G.E., Vermeylen, F.M., Stunder, B.J.B., 2005. The relation between NO_x emissions and precipitation NO_3^- in the eastern USA. Atmospheric Environment 37, 2093–2104.

Chamberlain, A.C., 1966. Transport of *Lycopodium* spores and other small particles to rough surfaces. Proceedings of the Royal Society of London 296A, 45–70.

Dämmgen, U., Zimmerling, R., 2002. Vertical fluxes of air-borne acidifying and eutrophying species in the Schorfheide Nature Reserve in Brandenburg, Germany. Journal of Applied Botany 76, 190–202.

Dorsey, J.R., Duyzer, J.H., Gallagher, M.W., Coe, H., Pilegaard, K., Weststrate, J.G., Jensen, N.O., Walton, S., 2004. Oxidized nitrogen and ozone interaction with forests. I: experimental observations and analysis of exchange with Douglas fir. Quarterly Journal of the Royal Meteorological Society 130, 1941–1955.

Duyzer, J.H., Dorsey, J.R., Gallagher, M.W., Pilegaard, K., Walton, S., 2004. Oxidized nitrogen and ozone interaction with forests. II: multi-layer process-oriented modelling results and a sensitive study for Douglas fir. Quarterly Journal of the Royal Meteorological Society 130, 1957–1971.

Dyer, A.J., Hicks, B.B., 1970. Flux–gradient relationships in the constant flux layer. Quarterly Journal of the Royal Meteorological Society 96, 715–721.

EC-UN/ECE (1996). Forest condition in Europe: Results of the 1995 Survey. European Commission (EC) and United Nations Economic Commission for Europe (UN/ECE), Brussels.

Erisman, J.W., Van Pul, A., Wyers, P., 1994. Parameterization of surface resistance for the quantification of atmospheric deposition of acidifying pollutants and ozone. Atmospheric Environment 28, 2595–2607.

Erisman, J.W., Vermeulen, A., Hensen, A., Flechard, C., Dämmgen, U., Fowler, D., Sutton, M., Grunhage, L., Tuovinen, J.P., 2005. Monitoring and modelling of biosphere/atmosphere exchange of gases and aerosols in Europe. Environmental Pollution 133, 403–413.

Eyckmans, K., Deutsch, F., Van Grieken, R., 2001. Measurements of Ammonia, Nitric Acid, Nitrous Acid and Small Aerosols at the Measuring Tower in Brasschaat 7,9,10/2000. UIA (in Dutch).

Ferm, M., Hultberg, H., 1999. Dry deposition and internal circulation of nitrogen, sulphur and base cations to coniferous forest. Atmospheric Environment 33, 4421–4430.

Fowler, D., Flechard, C., Skiba, U., Coyle, M., Cape, J.N., 1998. The atmospheric budget of oxidized nitrogen and its role in ozone formation and deposition. New Phytologist 139, 11–23.

Fowler, D., Muller, J., Smith, R.I., Cape, J.N., Erisman, J.W., 2005. Nonlinearities in source receptor relationships for sulfur and nitrogen compounds. Ambio 34, 41–46.

Gallagher, M.W., Beswick, K.M., Duyzer, J., Westrate, H., Choularton, T.W., Hummelshøj, P., 1997. Measurements of aerosol fluxes to Speulder forest using a micrometeorological technique. Atmospheric Environment 31, 359–373.

Garland, J.A., 1978. Dry and wet removal of sulfur from the atmosphere. Atmospheric Environment 12, 349–362.

Göckede, M., Mauder, M., Foken, T., 2005. Report on Results for the Site Brasschaat (BE-Bra). Department of Micrometeorology, University of Bayreuth, 16 pp.

Harrison, R.M., Pio, C.A., 1983. Size-differentiated composition of inorganic atmospheric aerosols of both marine and polluted continental origin. Atmospheric Environment 17, 1733–1738.

Harrison, R.M., Peak, J.D., Collins, G.M., 1996. Tropospheric cycle of nitrous acid. Journal of Geophysical Research 101, 14429–14439.

Hicks, B.B., Baldocchi, D.D., Meyers, T.P., Hosker, R.P., Matt, D.R., 1987. A preliminary multiple resistance routine for deriving dry deposition velocities from measured quantities. Water, Air, and Soil Pollution 36, 311–330.

Horii, C.V., Munger, J.W., Wofsy, S.C., Zahniser, M., Nelson, D., MacManus, J.B., 2004. Fluxes of nitrogen oxides over a temperate deciduous forest. Journal of Geophysical Research 109, 1–20.

Horváth, L., 2003. Dry deposition velocity of $PM_{2.5}$ ammonium sulfate particles to a Norway spruce forest on the basis of S- and N-balance estimations. Atmospheric Environment 37, 4419–4424.

Kleffmann, J., Kurtenbach, R., Lorzer, J., Wiesen, P., Kalthoff, N., Vogel, B., Vogel, H., 2003. Measured and simulated vertical profiles of nitrous acid – part I: field measurements. Atmospheric Environment 37, 2949–2955.

Koutrakis, P., Wolfson, J.M., Slater, J.L., Brauer, M., Spengler, J.D., 1988. Evaluation of an annular denuder/filter pack system to collect acidic aerosols and gases. Environmental Science and Technology 22, 1463–1468.

Koutrakis, P., Sioutas, C., Feruson, S.T., Wolfson, J.M., 1993. Development and evaluation of a glass honeycomb denuder/filter pack system to collect atmospheric gases and particles. Environmental Science and Technology 27, 2497–2501.

Kurtenbach, R., Becker, K.H., Gomes, J.A.G., Kleffmann, J., Lorzer, J.C., Spittler, M., Wiesen, P., Ackermann, R., Geyer, A., Platt, U., 2001. Investigations of emissions and heterogeneous formation of HONO in a road traffic tunnel. Atmospheric Environment 35, 3385–3394.

Langmuir, I., 1961. Mathematical investigation of water droplet trajectories. In: Suits, C.G., Way, H.E. (Eds.), The Collected Works of Irving Langmuir. Pergammon Press, New York, pp. 335–393.

Lenschow, D.H., 1982. Reactive trace species in the boundary layer from a micrometeorological perspective. Journal of the Meteorological Society of Japan 60, 472–480.

Lindberg, S.E., Lovett, G.M., Richter, D.D., Johnson, D.W., 1986. Atmospheric deposition and canopy interactions of major ions in a forest. Science 231, 141–145.

Lorenz, M., Fischer, R., Becher, G., Mues, V., Seidling, W., Kraft, Ph., Nagel, H.D., 2006. Forest Condition in Europe. Technical Report of ICP Forests. UNECE, Geneva, 131 pp.

Lovett, G.M., Lindberg, S.E., 1986. Dry deposition of nitrate to a deciduous forest. Biogeochemistry 2, 137–148.

Lovett, G.M., Lindberg, S.E., 1993. Atmospheric deposition and canopy interactions of nitrogen in forests. Canadian Journal of Forest Research 23, 1603–1616.

Lovett, G.M., 1994. Atmospheric deposition of nutrients and pollutants in North America: an ecological perspective. Ecological Applications 4, 629–650.

Marques, M.C., Gravenhorst, G., Ibrom, A., 2001. Input of atmospheric particles into forest stands by dry deposition. Water, Air and Soil Pollution 130, 571–576.

Meyers, T.P., Huebert, B.J., Hicks, B.B., 1989. HNO_3 deposition to a deciduous forest. Boundary-Layer Meteorology 49, 395–410.

Neirynck, J., Genouw, G., Coenen, S., Roskams, P., 2004. Depositions and Air Quality in Flemish Forests. Communications Institute for Forestry and Game Management. 2004/1 (in Dutch).

Neirynck, J., Kowalski, A., Carrara, A., Ceulemans, R., 2005. Driving forces for ammonia fluxes over mixed forest subjected to high deposition loads. Atmospheric Environment 39, 5013–5024.

Pryor, S.C., Barthelmie, R.J., Jensen, B., Jensen, N.O., Sorensen, L.L., 2002. HNO_3 fluxes to a deciduous forest derived using gradient and REA methods. Atmospheric Environment 36, 5993–5999.

Pryor, S.C., Klemm, O., 2004. Experimental derived estimates of nitric acid dry deposition velocity and viscous sub-layer resistance at a conifer forest. Atmospheric Environment 38, 2769–2777.

Reisinger, A.R., 2000. Observations of HNO_2 in the polluted winter atmosphere: possible heterogeneous production on aerosols. Atmospheric Environment 34, 3865–3874.

Ruijgrok, W., Tieben, H., Eisinga, P., 1997. The dry deposition of particles to a forest canopy: a comparison of model and experimental results. Atmospheric Environment 31, 399–415.

Saxén, B., Saxén, H., 1995. NNDT – A Neural Network Development Tool. Version 1.2.. Åbo Akademi University, Åbo, Finland

Schaap, M., Müller, K., ten Brink, H.M., 2002. Constructing the European aerosol nitrate concentration field from quality analysed data. Atmospheric Environment 36, 1323–1335.

Schmitt, M., Thöni, L., Waldner, P., Thimonier, A., 2005. Total deposition of nitrogen on Swiss long-term forest ecosystem research (LWF) plots: comparison of the throughfall and the inferential method. Atmospheric Environment 39, 1079–1091.

Sievering, H., Kelly, T., McConville, G., Seibold, C., Turnipseed, A., 2001. Nitric acid dry deposition to conifer forests: Niwot Ridge spruce–fir–pine study. Atmospheric Environment 35, 3851–3859.

Seinfeld, J.H., Pandis, S.N., 1998. Atmospheric Chemistry and Physics. From Air Pollution to Climate Change. J Wiley, New York.

Slinn, W.G.N., 1982. Predictions for particle deposition to vegetative surfaces. Atmospheric Environment 16, 1784–1794.

Staelens, J., De Schrijver, A., Van Avermaet, P., Genouw, G., Verhoest, N., 2005. A comparison of bulk and wet-only deposition at two adjacent sites in Melle (Belgium). Atmospheric Environment 39, 7–15.

Sutton, M.A., Burkhardt, J.K., Guerin, D., Nemitz, E., Fowler, D., 1998. Development of resistance models to describe measurements of bi-directional ammonia surface–atmosphere exchange. Atmospheric Environment 32, 473–480.

Sutton, M.A., Asman, W.A.H., Ellermann, T., Van Jaarsveld, J.A., Acker, K., Aneja, V., Duyzer, J., Horvath, L., Paramonov, S., Mitosinkova, M., Tang, Y.S., Achermann, B., Gauger, T., Bartniki, J., Neftel, A., Erisman, J.W., 2003. Establishing the link between ammonia emission control and measurements of reduced nitrogen concentrations and deposition. Environmental Monitoring and Assessment 82, 149–185.

Tarnay, L.W., Gertler, A., Taylor, G.E., 2002. The use of inferential models for estimating nitric acid vapor deposition to semi-arid coniferous forests. Atmospheric Environment 36, 3277–3287.

Thom, A.S., 1975. Momentum, mass, and heat exchange of plant communities. In: Monteith, L.L. (Ed.), Vegetation and the Atmosphere. Vol. I. Academic Press, London, pp. 57–109.

Ulrich, B., 1983. Interactions of forest canopies with atmospheric constituents: SO_2, alkali and earth alkali cations and chloride. In: Ulrich, B., Pankrath, J. (Eds.), Effects of Accumulation of Air Pollutants in Forest Ecosystems. Reidel, Dordrecht, pp. 33–45.

Vilà-Guerau de Arellano, J., Duynkerke, P.G., 1992. Influence of chemistry on the flux-gradient relationships for the $NO–O_3–NO_2$ system. Boundary-Layer Meteorology 61, 375–387.

Wesely, M.L., 1989. Parameterization of surface resistances to gaseous dry deposition in regional-scale numerical models. Atmospheric Environment 23, 1293–1304.

Wyers, G.P., Vermeulen, A.T., Slanina, A., 1992. Measurement of dry deposition of ammonia on a forest. Environmental Pollution 75, 25–28.

Wyers, G.P., Otjes, R.P., Slanina, J., 1993. A continuous-flow denuder for the measurement of ambient concentrations and surface-exchange fluxes of ammonia. Atmospheric Environment 27A, 2085–2090.

Wyers, G.P., Veltkamp, A.C., Geusebroek, M., Wayers, A., Möls, J.J., 1995. Deposition of aerosol to coniferous forest. In: Heij, G.J., Erisman, J.W. (Eds.), Acid Rain Research: Do We Have Enough Answers?. Studies in Environmental Science, vol. 64 Elsevier, Amsterdam, pp. 127–138.

Wyers, G.P., Erisman, J.W., 1998. Ammonia exchange over coniferous forest. Atmospheric Environment 32, 441–451.

Yeatman, S.G., Spokes, L.J., Jickells, T.D., 2001. Comparisons of coarse-mode aerosol nitrate and ammonium at two polluted coastal sites. Atmospheric Environment 35, 1321–1335.

Zimmermann, F., Plessow, K., Queck, R., Bernhofer, C., Matschullat, J., 2006. Atmospheric N- and S-fluxes to a spruce forest-two modelling approaches (eastern Erzgebirge, Germany). Atmospheric Environment 40, 4782–4796.